Life Sciences 231 (2019) 116567

Contents lists available at ScienceDirect

Life Sciences

journal homepage: www.elsevier.com/locate/lifescie

Endogenous TRPC channels mediate Ca^{2+} signals and trigeminal synaptic plasticity induced by mGluR5

Dong-ho Youn*, Haein Weon

Department of Oral Physiology, School of Dentistry, Kyungpook National University, 2177, Dalgubeol-daero, Jung-gu, Daegu, 41940, Republic of Korea

ARTICLE INFO

Keywords:
Metabotropic glutamate receptor 5
GCamp2
Ca^{2+} signal
Canonical transient receptor potential
Cyclic adenosine diphosphate ribose
Spinal trigeminal nucleus caudalis
Synaptic plasticity

ABSTRACT

Aims: Metabotropic glutamate receptor 5 (mGluR5), a member of group I mGluR, exerts its effect via elevation of intracellular Ca^{2+} level. We here characterized Ca^{2+} signals in the tsA201 cells transfected with mGluR5 and investigated the role of passages for mGluR5-induced Ca^{2+} signals in synaptic plasticity.

Main methods: Using a genetically encoded Ca^{2+} indicator, GCamp2, Ca^{2+} signals were reliably induced by bath application of (*S*)-3,5-dihydroxyphenylglycine, the group I mGluR agonist, in the tsA201 cells transfected with mGluR5. Using whole-cell recordings in the substantia gelatinosa (SG) neurons of the spinal trigeminal subnucleus caudalis (Vc), excitatory postsynaptic currents were recorded by stimulating the trigeminal tract.

Key findings: Ca^{2+} signals were mediated by "classical" or "canonical" transient receptor potential (TRPC) channels, particularly TRPC1/3/4/6, but not TRPC5, naturally existing in the tsA201 cells. Interestingly, the induction of Ca^{2+} signals was independent of the phospholipase C signaling pathway; instead, it critically involves the cyclic adenosine diphosphate ribose/ryanodine receptor-dependent signaling pathway and only partially protein kinase C. On the other hand, both TRPC3 and TRPC4 mediated mGluR1/5-induced long-lasting potentiation of excitatory synaptic transmission from the trigeminal primary afferents to the SG neurons of the Vc.

Significance: This study demonstrates that endogenous TRPC channels contribute to mGluR5-induced Ca^{2+} signals in tsA201 cells and synaptic plasticity at excitatory synapses.

1. Introduction

Various extracellular signals from neighboring cells or environment can be transduced into a form of local or global calcium ion (Ca^{2+}) signals inside cell, which is critical for cellular responses and further intercellular communication. To date, a number of methods have been developed to measure the intracellular Ca^{2+} signals. Beside of small-molecule Ca^{2+} indicator, such as fura-2 and indo-1, genetically encoded Ca^{2+} indicators (GECIs) have been recently developed and applied to measure the Ca^{2+} signals in a variety of cell types. These GECIs basically use fluorescent proteins that change their fluorescence depending on free Ca^{2+} concentration ($[Ca^{2+}]$) and have numerous advantages in a methodological aspect, for example, a selective and long-term measurement of intracellular $[Ca^{2+}]$ in a subset of cells within an intact tissue or in a subcellular compartment of a single cell [1]. In addition, the GECIs can be applicable for high-throughput or high-content biomolecular screening by observing single or multiple cellular functions [2]. Therefore, the use of GECIs provides diverse versatile tools for Ca^{2+} dynamics and drug development.

Metabotropic glutamate receptor type 5 (mGluR5), a subtype of group I mGluRs, is a G protein-coupled receptor (GPCR) that is activated by glutamate and coupled to G protein $G\alpha_{q/11}$, resulting in an elevation of intracellular Ca^{2+} level via its second messenger system. The mGluR5 has been implicated in various neurological disorders including Alzheimer's disease [3], addiction [4,5], pain [6], and migraine [7]. Hence, there has been a great effort made in the development of mGluR5-specific inhibitors to treat those neurological disorders [7–9].

In this study, we used a GECI, GCamp2 [10], to measure changes of cytosolic $[Ca^{2+}]$ when mGluR5 is transiently transfected and activated in the tsA201 cell line. The Ca^{2+} signals in this heterologous expression system were characterized using various inhibitors for signaling pathways and "classical" or "canonical" transient receptor potential (TRPC) channels. In addition, we identified that blocking TRPC channels prevented the induction of long-lasting potentiation of excitatory synaptic transmission at trigeminal primary afferent synapses in the substantia gelatinosa (SG) of spinal trigeminal subnucleus caudalis (Vc) that is the first central area processing orofacial sensory information.

* Corresponding author.
E-mail address: dyoun@knu.ac.kr (D.-h. Youn).

https://doi.org/10.1016/j.lfs.2019.116567
Received 19 April 2019; Received in revised form 11 June 2019; Accepted 12 June 2019
Available online 13 June 2019
0024-3205/

2. Materials and methods

2.1. Culture and transfection of tsA201 cells

Dulbecco's modified Eagle's medium (DMEM; Sigma-Aldrich, St. Louis, MO, USA), supplemented by 10% fetal bovine serum, 100 units/ml penicillin, 100 μg/ml streptomycin, and 2 mM glutamine, was used to culture tsA201 cells. The cells were grown in an incubator at 37 °C with humidified 5% CO_2 and 95% air and were transiently transfected with equimolar ratios of cDNAs encoding GCamp2 [10] and mGluR5 [11] (total amount of cDNA, 1 μg). The transfection was performed following the manufacturer's instructions for Effectene transfection reagent (QIAGEN, CA, USA). Transfected cells were plated onto No. 1 glass coverslips (15 mm, Warner Instruments, CT, USA) and were subjected to Ca^{2+} imaging 1–2 days after the plating (i.e., 2–3 days after transfection).

2.2. Ca^{2+} imaging

Ca^{2+} imaging experiments were conducted in HEPES-buffered Hank's balanced salt (HHBS) solution (Thermofisher Scientific, Waltham, MA, USA) that had the following composition (in mM): 10 HEPES, 1.26 $CaCl_2$; 0.49 $MgCl_2$; 0.41 $MgSO_4$; 5.33 KCl; 0.44 KH_2PO_4; 4.17 $NaHCO_3$; 138 NaCl; 0.34 Na_2HPO_4; 5.56 D-glucose. Ca^{2+}-free HHBS solution was obtained by substituting EGTA (0.1 mM) with $CaCl_2$. A coverslip with cells was placed in a chamber which was mounted on the stage of an inverted epifluorescence microscope (Eclipse T*i*S microscope, Nikon, Tokyo, Japan). A xenon arc lamp (Lambda LS, Sutter Instrument, Novato, CA, USA) was used for a light source, and 20× (NA, 0.45) or 40× (NA, 0.60) Nikon Fluor objectives were used to observe Ca^{2+} signals generated by the GCamp2 (filter cube, 465–495 nm for excitation wavelength and 515–555 nm for emission). Ca^{2+} signals were photographed by a cooled charge-couple device (CCD) camera (Zyla 5.5 MP sCMOS, 2560 × 2160 pixels, 6.5 × 6.5 μm pixel size; Andor, Belfast, UK). Experiments were performed using MetaFluor software (Molecular Devices, Sunnyvale, CA, USA), whose online mode allowed control of a mechanical shutter and measurement of fluorescent intensity caused by intracellular Ca^{2+} rise. Images were taken every 2 s by using the software and were background-subtracted. The magnitudes of Ca^{2+} signals in individual cells are represented as the percentage of fluorescent signal change over initial fluorescent intensity (%$\Delta F/F_0$). Two to five cells are selected in a coverslip. Ionomycin (10 μM), the membrane-permeable Ca^{2+} ionophore, was applied at the end of experiment for a maximal Ca^{2+} signal. Data are reported as the mean ± standard error of the mean (SEM). Statistical comparisons were assessed using an unpaired Student's *t*-test (*P < 0.05, **P < 0.01 or ***P < 0.001).

2.3. Preparation of horizontal brain stem slices

The horizontal brainstem slices (400–450 μm) were prepared from 6 to 14 day-old Sprague-Dawley rats of either sex as described previously [12]. Briefly, the brain and part of the cervical spinal cord were removed by guillotining a rat under deep urethane anesthesia (1.5 g/kg, i.p.) and then immediately transferred into an ice-cold Krebs' solution (composition in mM: NaCl 117, KCl 3.6, $CaCl_2$ 2.5, $MgCl_2$ 1.2, NaH_2PO_4 1.2, $NaHCO_3$ 25, and glucose 11; pre-oxygenated with a mixture of 95% O_2 and 5% CO_2; pH 7.4). In a pre-oxygenated ice-cold Krebs' solution, only the brainstem remained and was glued upside down on the flat top of a hard-mounting cube-block that was firmly fixed to the bottom of a slice chamber. Then horizontal slices were cut using a Vibratome 1000^+ (Vibratome, St. Louis, MO, USA). After the first cut of the ventral part of the brainstem, two horizontal brainstem slices were cut and used. The prepared slices were transferred into a beaker with fresh pre-oxygenated Krebs' solution at room temperature and incubated for at least an hour with continuous oxygenation to wash the hazardous or bioactive molecules released from the preparation processes. A slice from either the right or the left side was submerged and fixed in a recording chamber for whole-cell patch-clamp recordings.

2.4. Blind whole-cell patch-clamp recordings

Blind whole-cell recordings with patch pipettes (borosilicate glass, TW150F; WPI, Sarasota, FL, USA) were performed to record SG neurons in the Vc. When viewed under a microscope (BX51WI, Olympus, Tokyo, Japan) with transmitted illumination (40×), the 'translucent' SG area of the Vc was distinguishable. The pipette's resistance was typically 8–12 MΩ when filled with an internal solution (composition in mM: 145 K-gluconate, 5 NaCl, 1 $MgCl_2$, 0.2 EGTA, 10 HEPES, 2 Mg-ATP, and 0.1 Na_3-GTP; pH 7.2). All recordings were made under continuous perfusion of the pre-oxygenated Krebs' solution (2–3 ml/min; at room temperature, 23-25 °C).

To evoke excitatory postsynaptic currents (EPSCs) in the SG of Vc, the trigeminal tract (Vt) was stimulated every 30 s using a tungsten bipolar concentric electrode (TM33CCINS; tip diameter, 3–4 μm; WPI, Sarasota, FL, USA) that was connected with a stimulator (Grass S88; Grass Instruments, West Warwick, RI, USA). The distance between a stimulated site and a recording site was typically 2–4 mm. Evoked EPSCs were recorded at a holding potential of −70 mV after the identification of whole-cell formation by the appearance of the capacitance transients upon voltage pulses (−5 mV). In this recording condition, evoked EPSCs were completely blocked by 10 μM 2,3-dioxo-6-nitro-1,2,3,4-tetrahydrobenzo[*f*]quinoxaline-7-sulfonamide (NBQX), an α-amino-3-hydroxy-5-methylisoxazole-4-propionic acid (AMPA)/kainate receptor antagonist, indicating that the synaptic responses are glutamatergic. Recordings were amplified with a Multiclamp 700A amplifier (MDS Inc., Toronto, Canada), sampled at 5–10 KHz, and filtered at 1–2 KHz. Data acquisitions were performed using pClamp software (version 10; MDS Inc., Toronto, Canada). After recording relatively stable amplitudes of evoked EPSCs for 5–10 min (baseline period), (*S*)-3,5-dihydroxyphenylglycine (DHPG, 10 μM), a selective group I mGluR agonist, was bath-applied for 5 min. For antagonist experiments, pre-perfusion of Krebs' solution containing an antagonist at a certain concentration started at least 20 min before the DHPG application. Only monosynaptically evoked EPSCs were analyzed in their peak amplitudes. Each peak amplitude of evoked EPSC was represented as the percentage to the averaged baseline control (before DHPG application) over time. Each point at a given time in time course graphs presented mean ± SEM (%). Statistical comparisons were made using the Student's *t*-test; statistical significance, $P < 0.05$ or $P < 0.01$.

2.5. Chemicals

2-Aminoethoxydiphenylborane (2-APB), 1-[(4-chlorophenyl)methyl]-2-(1-pyrrolidinylmethyl)-1*H*-benzimidazole hydrochloride (clemizole), 2-[1-(3-dimethylaminopropyl)indol-3-yl]-3-(indol-3-yl) maleimide (GF109203x), DHPG, GSMTx4, 1-[6-[[(17β)-3-methoxyestra-1,3,5(10)-trien-17-yl]amino]hexyl]-1*H*-pyrrole-2,5-dione (U73122), 1-[2-(4-methoxyphenyl)-2-[3-(4-methoxyphenyl)propoxy]ethyl]-1*H*-imidazole hydrochloride (SKF96365), 2-methyl-6-(phenylethynyl)pyridine hydrochloride (MPEP), 4-methyl-2-(1-piperidinyl)quinolone (ML204), 1-[4-[(2,3,3-trichloro-1-oxo-2-propen-1-yl)amino]phenyl]-5-(trifluoromethyl)-1*H*-pyrazole-4-carboxylic acid (Pyr3), thapsigargin, and ryanodine were purchased from Tocris Cookson (Bristol, United Kingdom). Nicotinamide was purchased from Sigma-Aldrich (St. Louis, MO, USA). Chemicals were dissolved as stock solutions (> 1000× concentrated than the final concentration) in distilled water or dimethylsulfoxide (DMSO).

3. Results

When DHPG (100 μM), the mGluR1/5 agonist, was bath-applied to

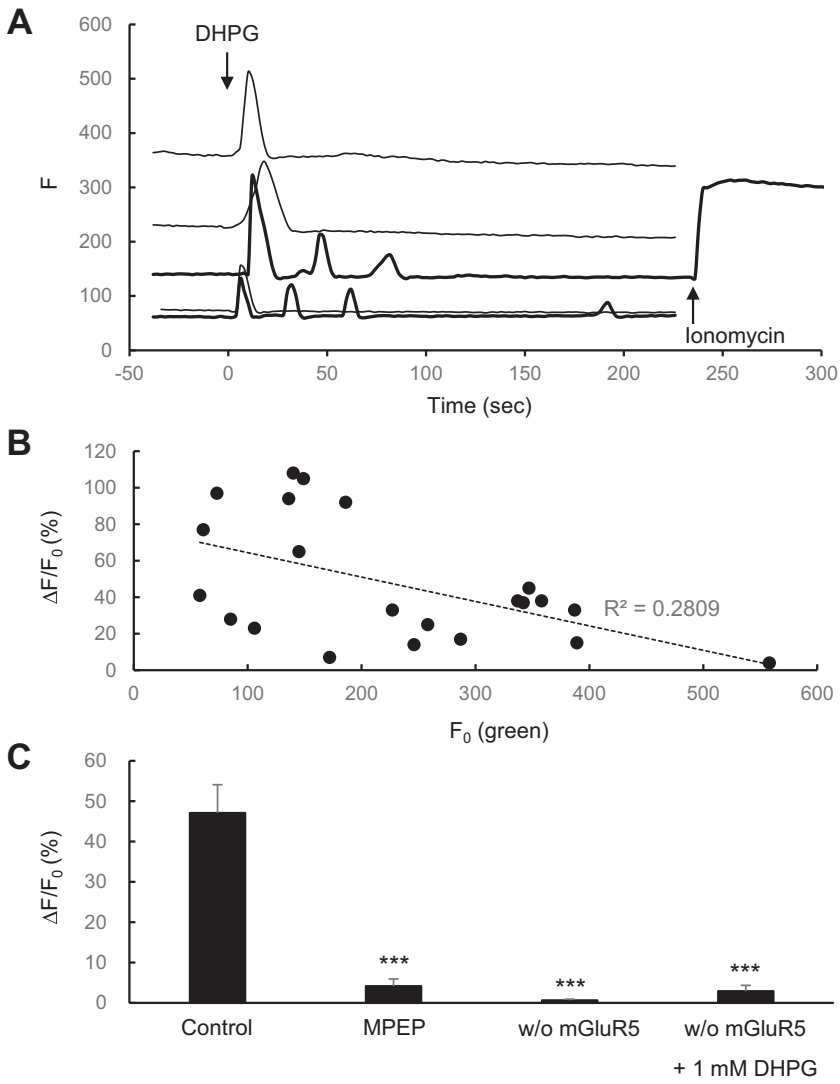

Fig. 1. Activation of mGluR5 generates intracellular Ca^{2+} signals in tsA201 cells expressing mGluR5 and GCamp2. (A) Traces for five representative tsA201 cells showing fluorescent changes upon the application of DHPG (100 μM), the group I mGluR agonist. tsA201 cells were transfected with cDNAs for mGluR5 and GCamp2, the genetically encoded Ca^{2+} indicator. Two cells (bold traces) exhibited more than two repetitive peaks. Ionomycin (10 μM), the Ca^{2+} ionophore, was applied in a cell. (B) A scatter plot of the percent change of fluorescent signal against the initial fluorescent intensity (F_0) from all tsA201 cells (n = 22). (C) A histogram shows a significant blockade of DHPG-induced fluorescent signals in the presence of MPEP (10 μM, n = 7), the selective mGluR5 antagonist, or no change of fluorescent signal without transfection of mGluR5 upon the application of DHPG (100 μM, n = 13; 1 mM, n = 11). ***P < 0.001 vs. control (n = 22).

activate mGluR5, an increased intensity of fluorescence appears in most of the fluorescent tsA201 cells that express GCamp2 and presumably mGluR5 (Fig. 1A). This type of Ca^{2+} signal was usually transient, lasting 10–30 s, and repeated several times within 5 min throughout the DHPG application (100 μM). Typically, there is a little correlation between the magnitudes of Ca^{2+} signals after bath-application of DHPG, expressed as $\%\Delta F/F_0$ (*see* Materials and Methods), and F_0 values in the range of 50 to 1000 within a region of interest ($R^2 = 0.28$; Fig. 1B), although there is a tendency for higher fluorescent changes when cells have low F_0. The magnitude of Ca^{2+} signals was 47.1 ± 7.0%ΔF/F_0 in twenty-two tsA201 cells selected (F_0, 229.4 ± 27.7; Fig. 1C). The Ca^{2+} signals were significantly blocked by the presence of MPEP (10 μM) before the application of DHPG (4.1 ± 1.8%ΔF/F_0, n = 7, ***P < 0.001; F_0, 39.4 ± 6.0), or did not appear when the mGluR5 plasmid was not co-expressed with the GCamp2 plasmid (without mGluR5: 100 μM DHPG, 0.6 ± 0.3%ΔF/F_0, 496.4 ± 122.9 of F_0, n = 13; 1 mM DHPG, 2.9 ± 1.5%ΔF/F_0, 215.8 ± 66.8 of F_0, n = 11).

To identify sources of cytosolic Ca^{2+} signals upon the activation of mGluR5 in tsA201 cells, Ca^{2+} was removed from the extracellular HBSS solution (*see* Materials and Methods). In this condition, bath-applied DHPG (100 μM) did not induce Ca^{2+} transients in the tsA201 cells expressing mGluR5 and GCamp2 (0.4 ± 1.5%ΔF/F_0, 216.9 ± 92.4 of F_0, n = 8; Fig. 2A and B), suggesting that the Ca^{2+} transients are actually due to the influx of Ca^{2+} through the plasma membrane of tsA201 cell. Because human embryonic kidney (HEK) 293 cells, the cell line before being transformed into the tsA201 cells with stable expression of an SV40 temperature-sensitive T antigens, endogenously express various types of TRPC channels [13–18], the possibility of TRPC channels is further tested for the influx of extracellular Ca^{2+}. In accordance with the endogenous expression of TRPC channels, the presence of SKF96365, the nonselective TRPC channel blocker, significantly prevented the induction of Ca^{2+} transients in the tsA201 cells expressing mGluR5 (0.7 ± 0.5%ΔF/F_0, 205.1 ± 71.9 of F_0, n = 14; Fig. 2B). Furthermore, the induction of Ca^{2+} transients was inhibited in the presence of selective TRPC blockers; GsMTx4 for TRPC1/6 (3.3 ± 1.2%ΔF/F_0, 194.3 ± 37.1 of F_0, n = 15), Pyr3 for TRPC3 (6.0 ± 1.4%ΔF/F_0, 232.9 ± 32.8 of F_0, n = 9), and ML204 for TRPC4 (13.9 ± 3.6%ΔF/F_0, 765.7 ± 100.1 of F_0, n = 6) (Fig. 2C). The inhibition was less in the presence of ML204, in comparison with the other two blockers. In contrast, the presence of clemizole, the antagonist for TRPC5 at a low concentration (below 10 μM) or for TRPC3/4/5/6 at a higher concentration (30 μM), did not prevent the induction of Ca^{2+} transients at the concentration of 2 μM (38.5 ± 10.3%ΔF/F_0, n = 13, P > 0.05 vs. control; 191.1 ± 33.7 of F_0; Fig. 3A and B), but did inhibit it at the concentration of 30 μM (3.6 ± 1.5%ΔF/F_0, n = 18, P < 0.05 vs. control; 175.1 ± 34.0 of F_0; Fig. 3B). These data clearly indicate that TRPC channels, except for TRPC5, endogenously expressing on the plasma membrane of tsA201 cells, mediate the Ca^{2+} transients upon the activation of mGluR5 transiently expressed in the tsA201 cells.

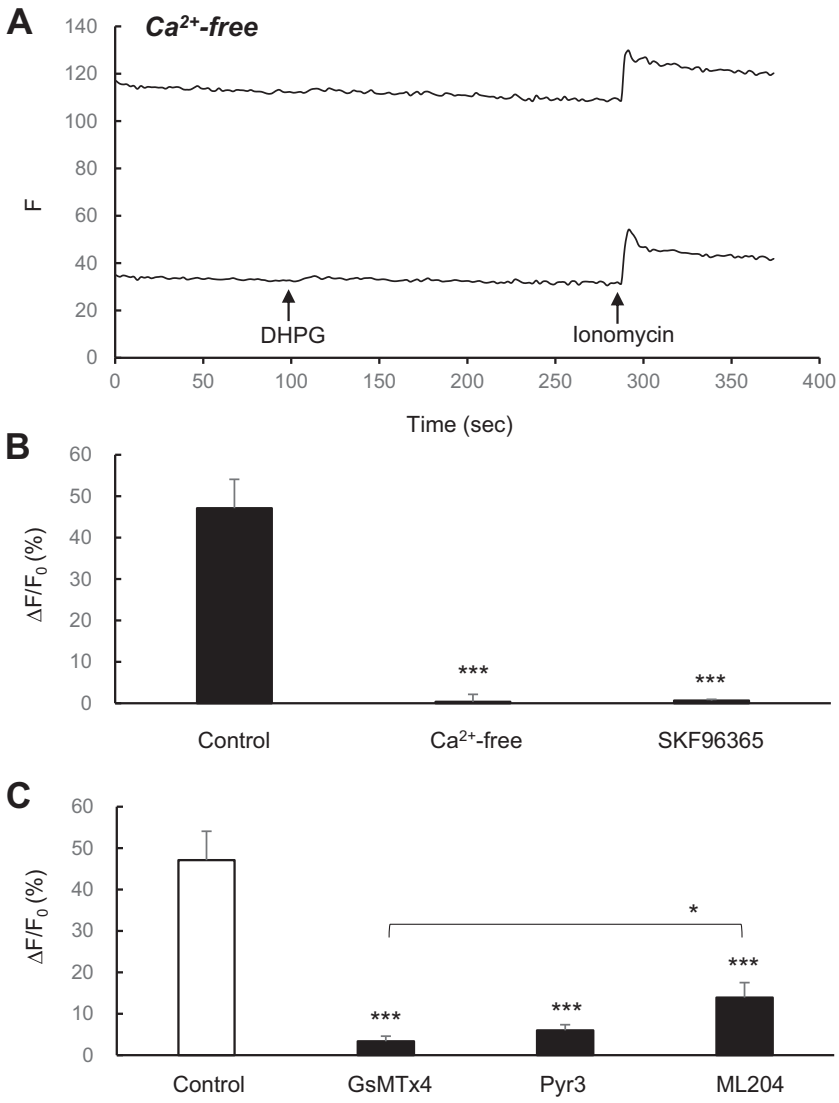

Fig. 2. Intracellular Ca^{2+} signals by the activation of mGluR5 in the mGluR5/GCamp2-expressing tsA201 cells are dependent on extracellular Ca^{2+} and various TRPC channels. (A) Representative traces for two tsA201 cells showing no fluorescent change upon the application of DHPG (100 μM) in the Ca^{2+}-free solution, but changes upon the application of ionomycin (10 μM), the Ca^{2+} ionophore. (B) A histogram shows significant blockade of fluorescent change in response to DHPG in the Ca^{2+}-free solution (n = 8) or in the presence of SKF96365 (n = 14), the nonselective TRPC channel blocker. ***P < 0.001 vs. control (n = 22). (C) A histogram demonstrates significant blockades of fluorescent change in response to DHPG application (100 μM) by the TRPC1/C6 blocker GsMTx4 (1 μM, n = 15), the selective TRPC3 blocker Pyr3 (10 μM, n = 9), or the selective TRPC4 blocker ML204 (10 μM, n = 6). ***P < 0.001 vs. control (n = 22). *P < 0.05 between GsMTx4 and ML204 groups.

The activation of mGluR5 leads to hydrolysis of phosphoinositides and generation of inositol 1,4,5-triphosphate (IP_3) and diacyl glycerol (DAG) via G_q/G_{11}-mediated phospholipase C (PLC) [19]. DAG further activates protein kinase C (PKC), and IP_3 recruits Ca^{2+} from intracellular Ca^{2+} stores via IP_3 receptor (IP_3R). Accordingly, this classical signaling pathway of mGluR5 was investigated for the TRPC-mediated Ca^{2+} transients by mGluR5 activation in the heterologous expression system of tsA201 cells. Unexpectedly, the Ca^{2+} transients were induced in the presence of U73122 (10 μM), the PLC inhibitor (Fig. 4A), and the averaged magnitude of Ca^{2+} transient was not significantly changed (53.2 ± 9.9%$\Delta F/F_0$, n = 18, P > 0.05 vs. control; 144.7 ± 32.0 of F_0; Fig. 4B). Moreover, GF109203x (1 μM), the PKC inhibitor, significantly but only partially inhibited the induction of Ca^{2+} signals (16.8 ± 7.4%$\Delta F/F_0$, n = 16, P < 0.01 vs. control; 328.1 ± 73.1 of F_0; Fig. 4B). In contrast, the induction of Ca^{2+} transients was completely blocked when the intracellular Ca^{2+} stores were depleted by thapsigargin (1 μM), the sarco/endoplasmic reticulum Ca^{2+} ATPase (SERCA) inhibitor (0.9 ± 0.2%$\Delta F/F_0$, 193.8 ± 26.2 of F_0, n = 17) or when IP_3R, a passage for the release of Ca^{2+} from the intracellular Ca^{2+} stores, was blocked by 2-APB (100 μM; 1.4 ± 0.6%$\Delta F/F_0$, 135.6 ± 23.5 of F_0, n = 13), indicating a significant role for IP_3R-mediated Ca^{2+} release from intracellular stores in the induction of Ca^{2+} transients. Since the Ca^{2+} signals did not depend on PLC in the present study, we further tested the PLC-independent pathway that uses cyclic adenosine diphosphate ribose (cADPR) to open ryanodine receptor (RyR) for Ca^{2+} release from intracellular stores [20,21]. As a result, the induction of Ca^{2+} signals was prominently inhibited by the blockades of RyR by ryanodine (20 μM), the RyR inhibitor (0.1 ± 0.1%$\Delta F/F_0$, 558.7 ± 89.5 of F_0, n = 14), or cADPR production by nicotinamide (5 mM), the inhibitor of ADP-ribosyl cyclase (4.6 ± 1.5%$\Delta F/F_0$, 927.8 ± 244.3 of F_0, n = 10) (Fig. 4B). Taken together, these results suggest that the Ca^{2+} signals induced by the activation of transiently-expressed mGluR5 in tsA201 cells require PLC-independent, but IP_3R- and cADPR/RyR-dependent signaling pathways.

Further, we investigated if TRPC channels involved a form of synaptic plasticity that is mediated by mGluR1/5. In the excitatory synaptic transmission from primary afferents of the Vt to the SG neurons of Vc, bath-applied DHPG (10 μM, 5 min) induced long-lasting potentiation of EPSC peak amplitude (123.7 ± 11.0% of baseline at 12 min, n = 6; Fig. 5). This type of synaptic plasticity was significantly prevented by the presence of the nonselective TRPC channel blocker SKF96365 (30 μM, 96.0 ± 3.3% of baseline at 12 min, n = 6, P < 0.05 vs. without antagonist), the selective TRPC3 blocker Pyr3 (10 μM, 91.3 ± 7.5% of baseline at 12 min, n = 6, P < 0.05 vs. without antagonist) or the selective TRPC4 blocker ML204 (10 μM, 87.5 ± 5.8% of baseline at 12 min, n = 6, P < 0.01 vs. without antagonist) (Fig. 5).

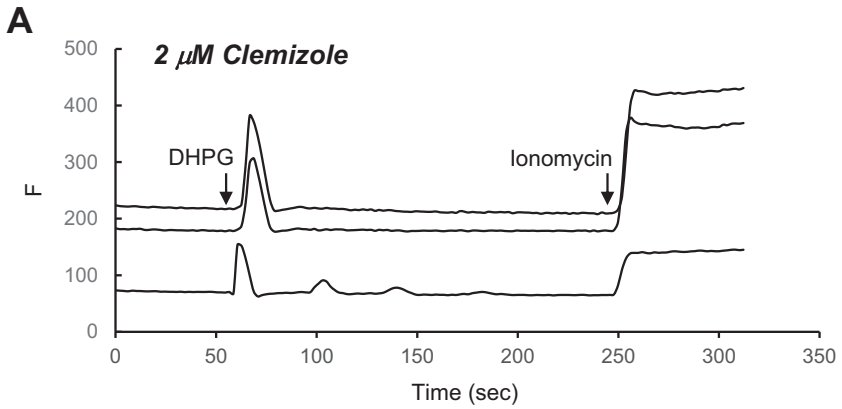

Fig. 3. No contribution of TRPC5 channels to the intracellular Ca^{2+} signals by the activation of mGluR5. (A) Representative traces for three tsA201 cells showing fluorescent change upon the application of DHPG (100 μM) in the presence of clemizole (2 μM), the antagonist for TRPC5 at a concentration of below 10 μM or for TRPC5 and other TRPC4/3/6 at a concentration of 30 μM. Application of ionomycin (10 μM), the Ca^{2+} ionophore, induces large and sustained fluorescent changes. (B) The DHPG-induced Ca^{2+} signal was not prevented by the presence of clemizole at the concentration of 2 μM or 10 μM, but prevented at the concentration of 30 μM (***P < 0.001).

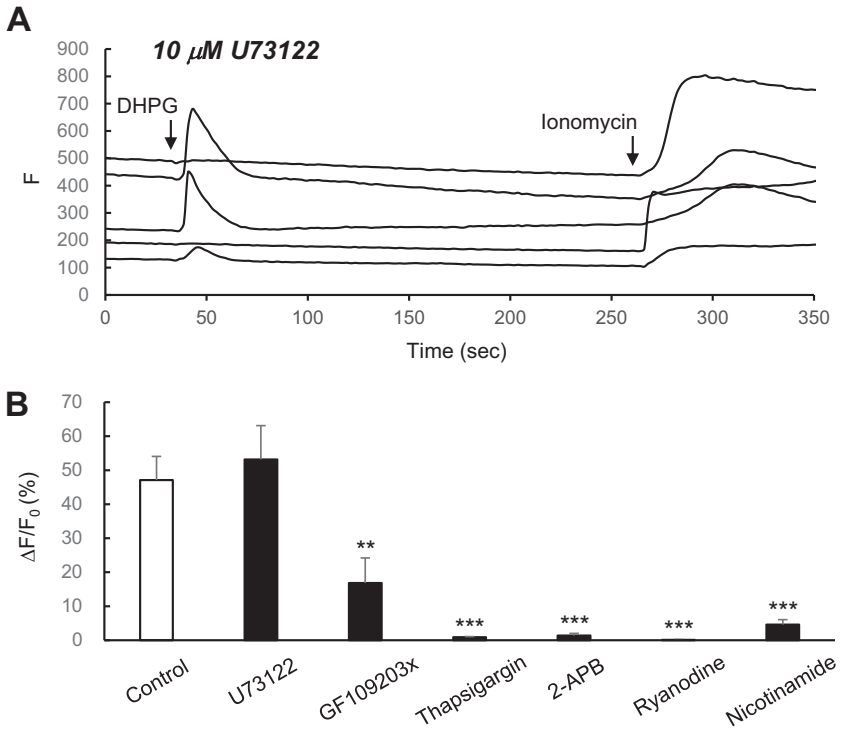

Fig. 4. Phospholipase C-independent and ADP-ribosyl cyclase-dependent pathway of mGluR5/TRPC-mediated Ca^{2+} signals in the tsA201 cells transfected with mGluR5. (A) Representative traces for three out of five tsA201 cells showing fluorescent change upon the application of DHPG (100 μM) in the presence of U73122 (10 μM), the phospholipase C inhibitor. Ionomycin (10 μM) was applied at the end of the experiment. (B) A summary histogram shows no inhibition in the presence of U73122, but significant changes in the presence of other inhibitors of signaling molecules, such as PKC (GF109203x, 1 μM), SERCA (thapsigargin, 1 μM), IP_3 receptor (2-APB, 100 μM), ryanodine receptor (ryanodine, 20 μM) and ADP-ribosyl cyclase (nicotinamide, 5 mM). **P < 0.01; ***P < 0.001.

4. Discussion

Using GCamp2 as a GECI, this study characterized Ca^{2+} signals induced by the activation of mGluR5 transiently expressed in the tsA201 cells. The Ca^{2+} signals were usually transient and repeated several times during the application of DHPG that activates mGluR5, and were mediated by an influx of Ca^{2+} through naturally-existing TRPC channels in the tsA201 cells, particularly TRPC1, 3, 4 and 6. Instead of a classical PLC-dependent pathway, PLC-independent and IP_3R- and cADPR/RyR-dependent signaling pathways mediate the induction of Ca^{2+} signals. In addition, this study demonstrated that naturally-existing TRPC3 and TRPC4 in the SG of the Vc contributed to mGluR1/5-induced long-lasting potentiation at excitatory synapses of the trigeminal primary afferents.

In this study, without transfection of mGluR5 cDNA plasmid to the tsA201 cells, Ca^{2+} signals were not induced, supporting no endogenous expression of mGluR5 in the tsA201 cells [22]. Additionally, although the agonist used in the study could activate both mGluR1 and mGluR5,

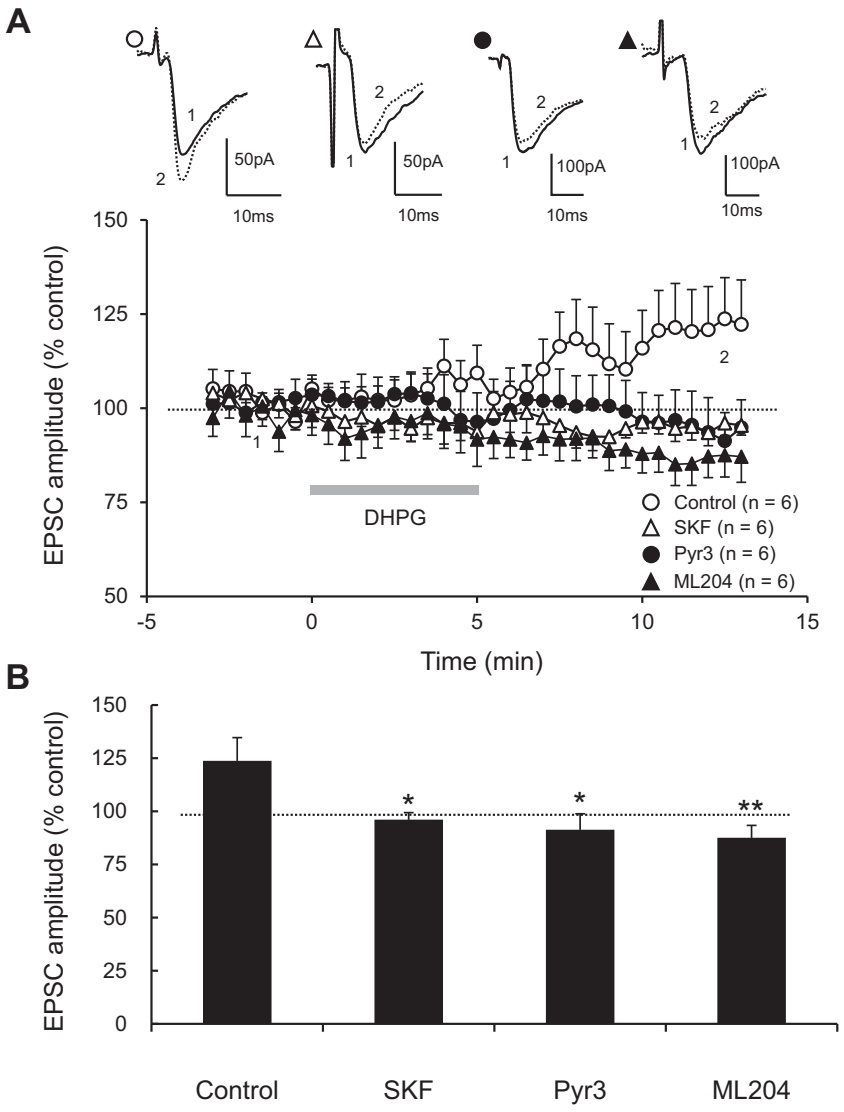

Fig. 5. Blockades of DHPG-induced long-lasting potentiation of excitatory synaptic transmission in the substantial gelatinosa of spinal trigeminal nucleus caudalis. (A) The induction of long-lasting potentiation of EPSCs by bath-applied DHPG (10 μM, 5 min, n = 6) was prevented by the presence of the nonselective TRPC channel blocker SKF96365 (30 μM, n = 6), the selective TRPC3 blocker Pyr3 (10 μM, n = 6) or the selective TRPC4 blocker ML204 (10 μM, n = 6). *Insets*, representative EPSC samples at the time indicated by the numbers above the time-course graph. (C) A summary histogram shows significant inhibition of the long-lasting potentiation in the presence of TRPC channel blockers. *P < 0.05; **P < 0.01.

the presence of the mGluR5 antagonist, MPEP, completely blocked the Ca^{2+} signals, eliminating the possibility of endogenous expression of mGluR1 in the tsA201 cells. On the other hand, HEK293 cells, the origin of tsA201 cells, express endogenously TRPC1, TRPC3, TRPC4, TRPC6 and TRPC7 proteins [14,15,17,18]. Likewise, in the present study, the Ca^{2+} signals were almost completely blocked by the inhibitor for TRPC1/6 (GsMTx4) and were partially but remarkably inhibited by the inhibitors for TRPC3 (Pyr3) or TRPC4 (ML204). In addition, the high concentration of clemizole (30 μM), which inhibits TRPC3/4/5/6, completely blocked the Ca^{2+} signal, whereas the low concentration of clemizole (2 μM), which inhibits only TRPC5, did not inhibit the signal. Therefore, our results, excluding the involvement of TRPC5 in the Ca^{2+} signals by mGluR5 activation, are in accordance with the studies demonstrating the expression pattern of TRPC channels in the HEK293 cells. Furthermore, the functional characterization of Ca^{2+} signals induced by the activation of mGluR5 will be useful for the study of TRPC channels in this heterologous expression system.

Interestingly, Ca^{2+} signals in the present study were not affected by the PLC inhibitor, but were inhibited partially by the PKC inhibitor and completely by both the depleting agent of intracellular Ca^{2+} stores and the inhibitors for IP_3R or RyR. These results suggest that a PLC-independent signaling pathway, as well as Ca^{2+} release from intracellular stores, is involved in the opening of TRPC channels when the mGluR5 is activated. Previous studies have reported that excitatory responses induced by activation of group I mGluRs involve PLC-independent pathways in hippocampal neurons [21,23] or cerebellar Purkinje neurons [24]. Instead of PLC, mGluR5-activated Ca^{2+} responses in the hippocampal neurons are mediated by a cADPR pathway and further RyR, but not by IP_3R [21]. Similarly, in the present study, the Ca^{2+} signals were blocked by inhibitors for cADPR-producing ADP-ribosyl cyclase or RyR. This result indicates the critical involvement of the cADPR/RyR signaling pathway in TRPC-mediated Ca^{2+} signals induced by activation of exogenous mGluR5 in the tsA201 cells.

On the other hand, the inhibitor of IP_3R, 2-APB, used in the present study, blocked the mGluR5-mediated Ca^{2+} signals. In addition, Ca^{2+} signals were blocked by the depletion of intracellular Ca^{2+} stores in the presence of an agent (thapsigargin) blocking SERCA. Although it is necessary to be further tested that 2-APB directly modulates TRPCs in the tsA201 cells [25], this result raises a possibility that a release of Ca^{2+} through IP_3R may be supportively involved in the Ca^{2+} signals [20], or the Ca^{2+} signals are indirectly involved in the modulation of IP_3R by cADPR-mediated enhancement of endoplasmic Ca^{2+} store filling [26]. Taken together, these results suggest that the activation of mGluR5 transiently expressed in the tsA201 cells recruits the cADPR-RyR, or apparently together with IP_3R, pathway, causing the Ca^{2+} release from the intracellular Ca^{2+} stores and further opening TRPC channels to produce the cytosolic Ca^{2+} signals. In this process, the depletion of intracellular Ca^{2+} stores may also be potentially involved

[27,28]. Recently, it has been demonstrated that stromal interaction molecule-1 (STIM1), an endoplasmic reticulum (ER) luminal Ca^{2+} sensor, plays a prominent role in store-operated Ca^{2+} entry (SOCE) [29,30]. STIM1 is moved to the junctions between ER and plasma membrane upon the Ca^{2+} release from, or the Ca^{2+} depletion of, intracellular stores [30]. At the junctions, STIM1 is associated with Orai1, a pore-forming subunit of channels on plasma membrane for SOCE [31], and activates TRPC channels that are recruited by Orai1 [27], resulting in Ca^{2+} influx. In the present study, the Ca^{2+} signals, only transiently induced by mGluR5 activation in the tsA201 cells, potentially employ the STIM1-Orai1-mediated pathway. In this view, it is likely that the transient Ca^{2+} signals require both Ca^{2+} release from intracellular stores and Ca^{2+} influx through TRPC channels, which would be eventually taken up for 'capacitative' Ca^{2+} entry into the stores [32]. Therefore, as shown in this study, the transient Ca^{2+} signals by mGluR5 activation would not be induced without extracellular Ca^{2+}, even if Ca^{2+} remained in the intracellular stores (Fig. 2A).

Because our results from the heterologous system suggests that the existence of TRPC channels contributes to the elevation of intracellular [Ca^{2+}] by the activation of mGluR5, we further investigate an involvement of TRPC channels in a form of synaptic plasticity mediated by the activation of group I mGluRs, i.e., mGluR1/5, in the Vc where an elevation of intracellular [Ca^{2+}] is required for mGluR5-dependent long-term synaptic plasticity [33]. The Vc is a central brain area for receiving sensory information, including pain, from orofacial area [12,34]. Blockades of TRPC3 or TRPC4 prevented the induction of long-lasting potentiation of trigeminal afferents-mediated excitatory synaptic transmission by the activation of group I mGluRs. In the dorsal root ganglion (DRG), an anatomical homology of the trigeminal ganglion, TRPC3 was found to be localized exclusively in small- and medium-diameter sensory neurons and contributed to the SOCE [35]. In addition, TRPC3 mediated Ca^{2+} and Na^{+}-carrying nonselective cation currents in the rat DRG neurons that are induced by IgG immune complex [36]. These previous studies together highlight the critical involvement of TRPC3 in Ca^{2+} homeostasis in the sensory neurons, potentially contributing to chronic pain. In this aspect, our results additionally demonstrate the significant contribution of both TRPC3 and TRPC4 to the mGluR1/5-mediated synaptic plasticity in the SG of Vc, suggesting a potential target of these nonselective cation channels for pathological pain conditions [37].

5. Conclusion

The present study shows that Ca^{2+} signals induced by the activation of mGluR5 transiently expressed in the tsA201 cells are mediated by Ca^{2+} influx through endogenous TRPC channels via the PLC-independent and cADPR/RyR-dependent signaling pathway. In addition, it is shown that both TRPC3 and TRPC4 contribute to mGluR1/5-induced synaptic plasticity at trigeminal excitatory synapses in the SG of the Vc.

Declaration of Competing Interest

The authors declare that there are no conflicts of interest.

Acknowledgments

This research was supported by Basic Science Research Program through the National Research Foundation of Korea (NRF), funded by the Ministry of Education (NRF-2018R1D1A1B07047469).

References

[1] A.E. Palmer, R.Y. Tsien, Measuring calcium signaling using genetically targetable fluorescent indicators, Nat. Protoc. 1 (2006) 1057–1065.
[2] J.J. Bassett, G.R. Monteith, Genetically encoded calcium indicators as probes to assess the role of calcium channels in disease and for high-throughput drug discovery, Adv. Pharmacol. 79 (2017) 141–171.
[3] A. Hamilton, M. Vasefi, C. Vander Tuin, R.J. McQuaid, H. Anisman, S.S. Ferguson, Chronic pharmacological mGluR5 inhibition prevents cognitive impairment and reduces pathogenesis in an Alzheimer disease mouse model, Cell Rep. 15 (2016) 1859–1865.
[4] C. Chiamulera, M.P. Epping-Jordan, A. Zocchi, C. Marcon, C. Cottiny, S. Tacconi, et al., Reinforcing and locomotor stimulant effects of cocaine are absent in mGluR5 null mutant mice, Nat. Neurosci. 4 (2001) 873–874.
[5] P.J. Kenny, B. Boutrel, F. Gasparini, G.F. Koob, A. Markou, Metabotropic glutamate 5 receptor blockade may attenuate cocaine self-administration by decreasing brain reward function in rats, Psychopharmacology 179 (2005) 247–254.
[6] V. Pereira, C. Goudet, Emerging trends in pain modulation by metabotropic glutamate receptors, Front. Mol. Neurosci. 11 (2019) 464.
[7] M.W. Waung, S. Akerman, M. Wakefield, C. Keywood, P.J. Goadsby, Metabotropic glutamate receptor 5: a target for migraine therapy, Ann Clin Transl Neurol 3 (2016) 560–571.
[8] T.M. Keck, M.F. Zou, G.H. Bi, H.Y. Zhang, X.F. Wang, H.J. Yang, et al., A novel mGluR5 antagonist, MFZ 10-7, inhibits cocaine-taking and cocaine-seeking behavior in rats, Addict. Biol. 19 (2014) 195–209.
[9] P.M.t. Lea, A.I. Faden, Metabotropic glutamate receptor subtype 5 antagonists MPEP and MTEP, CNS Drug Rev 12 (2006) 149–166.
[10] Y.N. Tallini, M. Ohkura, B.R. Choi, G. Ji, K. Imoto, R. Doran, et al., Imaging cellular signals in the heart in vivo: cardiac expression of the high-signal Ca2+ indicator GCaMP2, Proc. Natl. Acad. Sci. U. S. A. 103 (2006) 4753–4758.
[11] T. Abe, H. Sugihara, H. Nawa, R. Shigemoto, N. Mizuno, S. Nakanishi, Molecular characterization of a novel metabotropic glutamate receptor mGluR5 coupled to inositol phosphate/Ca2+ signal transduction, J. Biol. Chem. 267 (1992) 13361–13368.
[12] H. Weon, T.W. Kim, D.H. Youn, Postsynaptic N-type or P/Q-type calcium channels mediate long-term potentiation by group I metabotropic glutamate receptors in the trigeminal oralis, Life Sci. 188 (2017) 110–117.
[13] V. Bugaj, V. Alexeenko, A. Zubov, L. Glushankova, A. Nikolaev, Z. Wang, et al., Functional properties of endogenous receptor- and store-operated calcium influx channels in HEK293 cells, J. Biol. Chem. 280 (2005) 16790–16797.
[14] R.L. Garcia, W.P. Schilling, Differential expression of mammalian TRP homologues across tissues and cell lines, Biochem. Biophys. Res. Commun. 239 (1997) 279–283.
[15] K. Groschner, S. Hingel, B. Lintschinger, M. Balzer, C. Romanin, X. Zhu, et al., Trp proteins form store-operated cation channels in human vascular endothelial cells, FEBS Lett. 437 (1998) 101–106.
[16] J.P. Lievremont, G.S. Bird, J.W. Putney, Jr., Canonical transient receptor potential TRPC7 can function as both a receptor- and store-operated channel in HEK-293 cells, Am J Physiol Cell Physiol 287 (2004) C1709–1716.
[17] X. Wu, G. Babnigg, T. Zagranichnaya, M.L. Villereal, The role of endogenous human Trp4 in regulating carbachol-induced calcium oscillations in HEK-293 cells, J. Biol. Chem. 277 (2002) 13597–13608.
[18] T.K. Zagranichnaya, X. Wu, M.L. Villereal, Endogenous TRPC1, TRPC3, and TRPC7 proteins combine to form native store-operated channels in HEK-293 cells, J. Biol. Chem. 280 (2005) 29559–29569.
[19] C.M. Niswender, P.J. Conn, Metabotropic glutamate receptors: physiology, pharmacology, and disease, Annu. Rev. Pharmacol. Toxicol. 50 (2010) 295–322.
[20] H. Morikawa, K. Khodakhah, J.T. Williams, Two intracellular pathways mediate metabotropic glutamate receptor-induced Ca2+ mobilization in dopamine neurons, J. Neurosci. 23 (2003) 149–157.
[21] J.W. Sohn, W.J. Yu, D. Lee, H.S. Shin, S.H. Lee, W.K. Ho, Cyclic ADP ribose-dependent Ca2+ release by group I metabotropic glutamate receptors in acutely dissociated rat hippocampal neurons, PLoS One 6 (2011) e26625.
[22] B.K. Atwood, J. Lopez, J. Wager-Miller, K. Mackie, A. Straiker, Expression of G protein-coupled receptors and related proteins in HEK293, AtT20, BV2, and N18 cell lines as revealed by microarray analysis, BMC Genomics 12 (2011) 14.
[23] D.R. Ireland, W.C. Abraham, Group I mGluRs increase excitability of hippocampal CA1 pyramidal neurons by a PLC-independent mechanism, J. Neurophysiol. 88 (2002) 107–116.
[24] M. Hirono, S. Konishi, T. Yoshioka, Phospholipase C-independent group I metabotropic glutamate receptor-mediated inward current in mouse purkinje cells, Biochem. Biophys. Res. Commun. 251 (1998) 753–758.
[25] S.Z. Xu, F. Zeng, G. Boulay, C. Grimm, C. Harteneck, D.J. Beech, Block of TRPC5 channels by 2-aminoethoxydiphenyl borate: a differential, extracellular and voltage-dependent effect, Br. J. Pharmacol. 145 (2005) 405–414.
[26] M. Yamasaki-Mann, A. Demuro, I. Parker, Modulation of endoplasmic reticulum Ca2+ store filling by cyclic ADP-ribose promotes inositol trisphosphate (IP3)-evoked Ca2+ signals, J. Biol. Chem. 285 (2010) 25053–25061.
[27] I.S. Ambudkar, L.B. de Souza, H.L. Ong, TRPC1, Orai1, and STIM1 in SOCE: friends in tight spaces, Cell Calcium 63 (2017) 33–39.
[28] J. Avila-Medina, I. Mayoral-Gonzalez, A. Dominguez-Rodriguez, I. Gallardo-Castillo, J. Ribas, A. Ordonez, et al., The complex role of store operated calcium entry pathways and related proteins in the function of cardiac, skeletal and vascular smooth muscle cells, Front. Physiol. 9 (2018) 257.
[29] J. Liou, M.L. Kim, W.D. Heo, J.T. Jones, J.W. Myers, J.E. Ferrell Jr.et al., STIM is a Ca2+ sensor essential for Ca2+ −store-depletion-triggered Ca2+ influx, Curr. Biol. 15 (2005) 1235–1241.
[30] S.L. Zhang, Y. Yu, J. Roos, J.A. Kozak, T.J. Deerinck, M.H. Ellisman, et al., STIM1 is a Ca2+ sensor that activates CRAC channels and migrates from the Ca2+ store to the plasma membrane, Nature 437 (2005) 902–905.
[31] S. Feske, Y. Gwack, M. Prakriya, S. Srikanth, S.H. Puppel, B. Tanasa, et al., A mutation in Orai1 causes immune deficiency by abrogating CRAC channel function,

Nature 441 (2006) 179–185.
[32] J.W. Putney, Jr., A model for receptor-regulated calcium entry, Cell Calcium 7 (1986) 1–12.
[33] Y.C. Liang, C.C. Huang, K.S. Hsu, Characterization of long-term potentiation of primary afferent transmission at trigeminal synapses of juvenile rats: essential role of subtype 5 metabotropic glutamate receptors, Pain 114 (2005) 417–428.
[34] D.H. Youn, Trigeminal long-term potentiation as a cellular substrate for migraine, Med. Hypotheses 110 (2018) 27–30.
[35] H. Alkhani, A.R. Ase, R. Grant, D. O'Donnell, K. Groschner, P. Seguela, Contribution of TRPC3 to store-operated calcium entry and inflammatory transductions in primary nociceptors, Mol. Pain 10 (2014) 43.
[36] L. Qu, Y. Li, X. Pan, P. Zhang, R.H. LaMotte, C. Ma, Transient receptor potential canonical 3 (TRPC3) is required for IgG immune complex-induced excitation of the rat dorsal root ganglion neurons, J. Neurosci. 32 (2012) 9554–9562.
[37] M. Xia, D. Liu, C. Yao, TRPC3: a new target for therapeutic strategies in chronic pain-DAG-mediated activation of non-selective cation currents and chronic pain (Mol Pain 2014;10:43), J Neurogastroenterol Motil 21 (2015) 445–447.